Cytotoxicity Effects of Graphene and Single-Wall Carbon Nanotubes in Neural Phaeochromocytoma-Derived PC12 Cells

Yongbin Zhang,[†] Syed F. Ali,[†,*] Enkeleda Dervishi,[‡] Yang Xu,[‡] Zhongrui Li,[‡] Daniel Casciano,[‡] and Alexandru S. Biris[‡,*]

[†]Neurochemistry Laboratory, Division of Neurotoxicology, National Center for Toxicological Research, Food and Drug Administration, 3900 NCTR Road, Jefferson, Arkansas 72079 and [‡]Nanotechnology Center, Applied Science Department, University of Arkansas at Little Rock, 2801 South University Avenue, Little Rock, Arkansas 72204

ABSTRACT Graphitic nanomaterials such as graphene layers (G) and single-wall carbon nanotubes (SWCNT) are potential candidates in a large number of biomedical applications. However, little is known about the effects of these nanomaterials on biological systems. Here we show that the shape of these materials is directly related to their induced cellular toxicity. Both G and SWCNT induce cytotoxic effects, and these effects are concentration- and shape-dependent. Interestingly, at low concentrations, G induced stronger metabolic activity than SWCNT, a trend that reversed at higher concentrations. Lactate dehydrogenase levels were found to be significantly higher for SWCNT as compared to the G samples. Moreover, reactive oxygen species were generated in a concentration- and time-dependent manner after exposure to G, indicating an oxidative stress mechanism. Furthermore, time-dependent caspase 3 activation after exposure to G (10 μg/mL) shows evidence of apoptosis. Altogether these studies suggest different biological activities of the graphitic nanomaterials, with the shape playing a primary role.

KEYWORDS: graphene · single-wall carbon nanotubes · cytotoxicity · shape · PC12 cells · reactive oxidative species

Graphitic nanomaterials—such as carbon nanotubes (CNT), fullerenes, and more recently graphene—have gained a great deal of interest in the scientific community due to their novel properties and wide range of potential applications. Graphene (G) has become one of the most intensively studied such nanomaterials for a number of applications. Studies focus on taking advantage of its chemical, physical, and other properties in order to develop novel applications with advanced scientific and commercial potential.[1−4] However, the biological applications and potential adverse effects of G remain almost completely unknown. Recently, G or graphite oxides sheets have received significant attention for their potential application in biology and medicine, including biodevices, microbial detection, disease diagnosis,[5] and drug delivery systems.[6] A key issue that needs to be investigated in the full implementation of such nanomaterials in a large range of biological applications and processes is their relatively unknown cytotoxicity and biological activity. Such studies would provide insight into the interaction between atomically flat graphitic structures and various biological systems both *in vitro* and *in vivo*. The cytotoxic effects of G are expected to be significantly different when compared to those of one-dimensional CNT, which have been widely studied.[7,8] Although the two materials have a similar chemical composition and crystalline structure, their shape is different (flat atomic sheets for G and tubular for nanotubes); as a result, their interactions with cell systems are expected to be governed by different mechanisms. Given the high potential of G structures to be used as delivery vehicles for growth factors and other proteins for neural reconstruction and regeneration of the nervous system (which is essential in the treatment of Alzheimer's disease), it is crucial to fully study and understand the interaction and the bioreactivity of such nanomaterials when exposed to neuronal cells. This article presents an evaluation of the *in vitro* toxicity of G by using neuronal PC12 cells compared to single-wall carbon nanotubes (SWCNT) in similar conditions. A clear difference in the toxic levels between G and SWCNT is indicated. To the best of our knowledge, this is the first study to address this issue.

G AND SWCNT SYNTHESIS

High quantities of few-layer G sheets were successfully synthesized on the Fe−Co/MgO (2.5:2.5:95 wt %) catalytic system utilizing the radio frequency catalytic

*Address correspondence to syed.ali@fda.hhs.gov, asbiris@ualr.edu

Received for review April 7, 2010 and accepted May 12, 2010.

Published online May 18, 2010. 10.1021/nn1007176

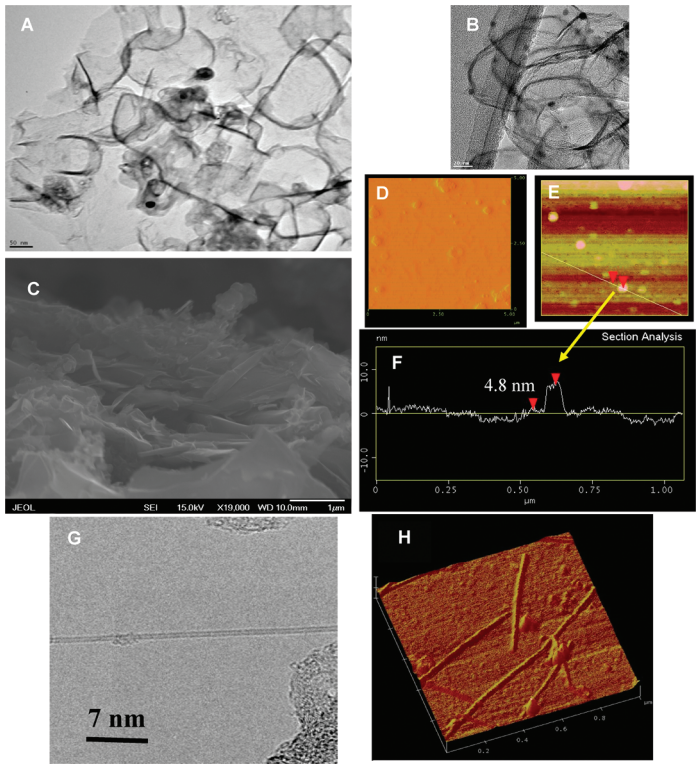

Figure 1. (A) Low-magnification TEM image of graphene sheets. (B) High-magnification TEM image of few-layer graphene sheets overlaid side-by-side. (C) SEM image of the semitransparent graphene sheets synthesized in large quantities. (D) High-pass filtered AFM scan of graphene sheets overlaid on the Si surface. (E) AFM image of the few-layer graphene sheets, with (F) a corresponding AFM height image. (G) High-resolution TEM image of the single-wall carbon nanotubes used for this study. (H) AFM images of the nanotubes used for this study. The diameter of the nanotubes ranged from 0.8 to 1.2 nm.

chemical vapor deposition (RF-cCVD) technique.[9] Figure 1A shows a low-magnification transmission electron microscopy (TEM) image of the as-produced G sheets. A high-magnification TEM image (Figure 1B) shows the overlaid side-by-side sheets, varying between 100 and 110 nm in diameter. Scanning electron microscopy (SEM) images (Figure 1C) reveal that most of the G sheets have only a few layers. Atomic force microscopy (AFM) was used to measure the thickness of the synthesized G nanosheets; the results are presented in Figure 1D,E. The height image shown in Figure 1F indicates that the thickness of the G sheets varies between 3 and 5 nm, corresponding to approximately 3−5 layers. Based on high-resolution microscopy analysis, approximately 80% of the G structures have 3−5 layers, 8% of them have 1−3 layers, and 12% have 6−10 layers.

Raman spectroscopy is a nondestructive technique that has been used to characterize the crystallinity and the number of G layers.[10,11] Raman spectroscopy measurements (not shown here) indicated the presence of the few-layer G sheets.[9] The full width at half-maximum (fwhm) of the 2D peak showed that the G presented in this work contains approximately 3−5 layers.[9,12] The X-ray diffraction (XRD) technique was used to analyze the crystallinity and estimate the number of layers in the G nanosheets. Using the values of the *d*-spacing and the size of crystallite, these G sheets were found to have, on average, 3−5 layers.[13,14] The XRD results were found to support microscopy and spectroscopy results, indicating the presence of very few-layer G sheets.[9]

Figure 1G,H shows representative high-magnification TEM and AFM images of the SWCNT used for these studies. The diameter of the nanotubes ranged from 0.8 to 1.2 nm. The purity of all the samples, both G and SWCNT, was higher than 98.5%. Zeta potential of CNT and G was measured using a ZETA-READER MARK 21 instrument (Zeta Potential Instruments, Inc., Bedminster, NJ) in either water or RPMI-1640 medium under the same exposure condition. Zeta potential of SWNT and G in water was −15.53 and −35.59 mV, respectively. However, the zeta potential value of these two nanomaterials changed to the same value, −8.5 mV, when they were dispersed in the medium. These data suggest that protein binding in the medium may affect the surface charge of these nanomaterials.

CYTOTOXICITY CHARACTERIZATION

Several studies suggested that nanomaterials elicit toxicity in cell cultures and in rodent models.[14−21] G, a promising material given its structure and properties, is expected to have significant applications in nanomedicine. Therefore, the cytotoxicity of highly pure SWCNT and G was measured and compared. The studies shown schematically in Figure 2 were focused on understanding the effect that the shape of these nanomaterials had on their corresponding cellular cytotoxicity.

MTT assay, a common method of evaluating the adverse effect of nanomaterials in cell culture, was used to measure the mitochondria function of the cells. After 24 h of exposure to either G or SWCNT, the metabolic activity of PC12 cells decreased in a concentration-dependent manner (Figure 3A). Interestingly, we found that the concentration-dependent toxicity of these two nanomaterials of relatively identical chemical struc-

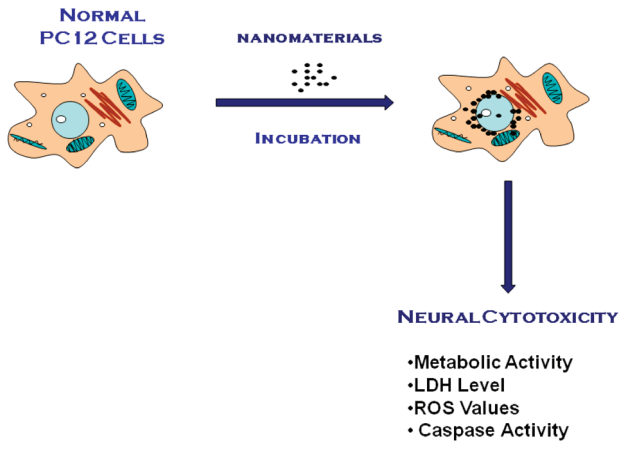

Figure 2. Schematic diagram showing the experimental conditions under which the shape of the graphitic nanomaterials (G and SWCNT) was investigated for the corresponding induced cytotoxic effects.

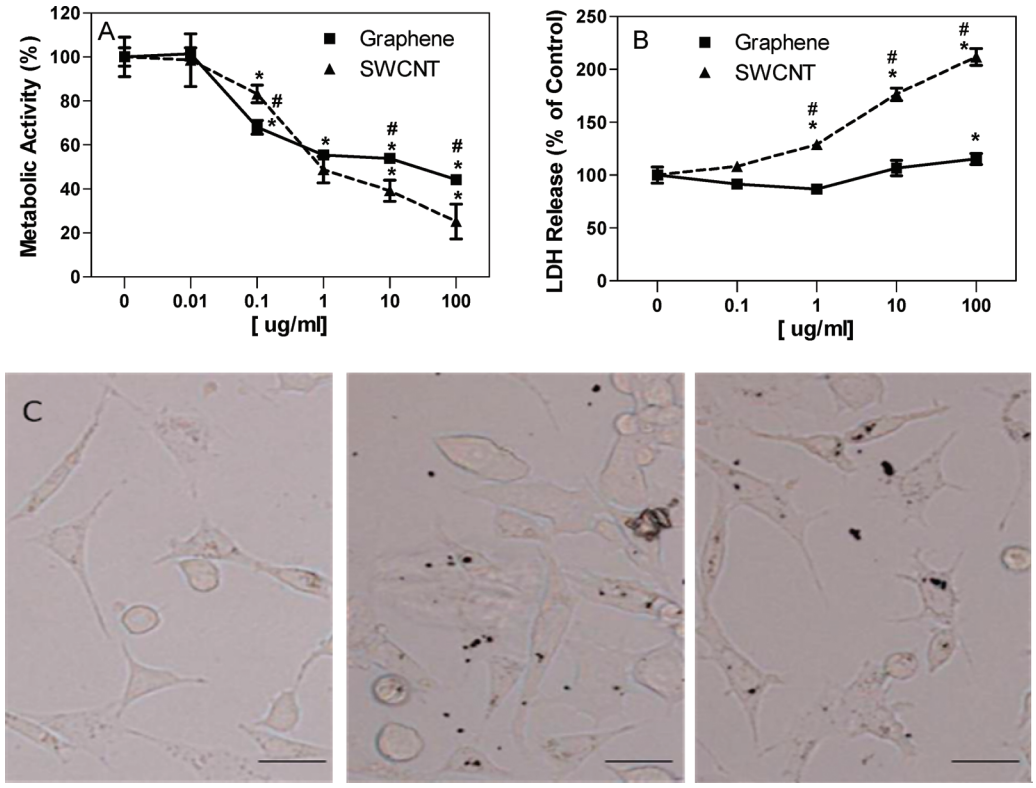

Figure 3. Effect of G or SWCNT on (A) mitochondrial toxicity and (B) LDH release (cell membrane damage marker). (C) Morphology change of PC12 cells: left, control; middle, G; right, SWCNT. Bar = 10 μm.

ture did not present a similar pattern, indicating a different toxic mechanism. The results indicate that, at low concentrations, the G structures induce a more intense toxic response than the SWCNT. As the concentration increases, the induced cytotoxic effects reverse, with the G showing a lower activity. These mitochondrial toxicity findings can be explained by the shape of these nanomaterials and their biological interaction with the cellular systems. As previously discussed, the "snaking" effects of the SWCNT, given their tubular shape, promote penetration of membranes, uptake by cells, and strong interactions with various protein systems.[22] Due to their flat shapes, the G nanostructures were expected to have even stronger interaction with the cellular membranes, indicating different cellular target sites for the two types of nanomaterials. It was reported previously that different degrees of agglomeration of SWCNT influence the DNA content in primary neuron and glial cells.[19] In current studies, aggregation/agglomeration of G sheets on the cell membranes after 24 h of incubation (Figure 3C) was expected to contribute at least partially to their toxic properties.

A number of studies show that nanomaterials could induce apoptosis or necrosis.[23,24] To evaluate the mechanism of cell death in PC12 cells induced by G sheets, two important enzymes were measured. Lactate dehydrogenase (LDH) release measures the membrane damage, a hallmark of necrosis, while caspase activation indicates apoptosis. In our studies, significant LDH release was noted only after 24 h of exposure to G at the highest concentration (100 μg/mL) (Figure 3B). At lower concentrations (0.01−10 μg/mL), G had no effect on the release of LDH. In contrast, SWCNT induced a dramatic release of LDH. A previous study investigating the effects of CNT on the lungs of rats indicated a higher response for the nanotubes when compared to quartz dust.[25] It is likely the needle-like CNT may be more mobile and can more easily penetrate the cell membrane, resulting in greater cell membrane damage. We also detected the effect of G on the morphology of the PC12 cells (Figure 3C): the cell membrane appears to be intact, but some small aggregates were noted on the surface of the cells, indicating membrane binding without damage. Oxidative stress is a common mechanism of nanomaterials, including carbon nanomaterials.[26,27] We explored the generation of reactive oxygen species (ROS) to determine if it were involved in the toxic mechanism of G sheet. Figure 4A shows the level of the generated ROS to be concentration- and time-dependent after exposure to G. Four hours after treatment, 100 μg/mL of G induced ROS 6-fold compared to control. The generated ROS levels were also significant for the 10 and 100 μg/mL groups after 24 h of G exposure. On the other hand, time-dependent caspase 3 activation indicated a weak caspase 3-mediated apoptotic pathway (Figure 4B).

It should be noted that the maximum exposure level of G (100 μg/mL) in our study is higher than the 30 μg/mL of other reported carbon-based nanomaterials.[28,29] It was reported that 7.5−30 μg/mL

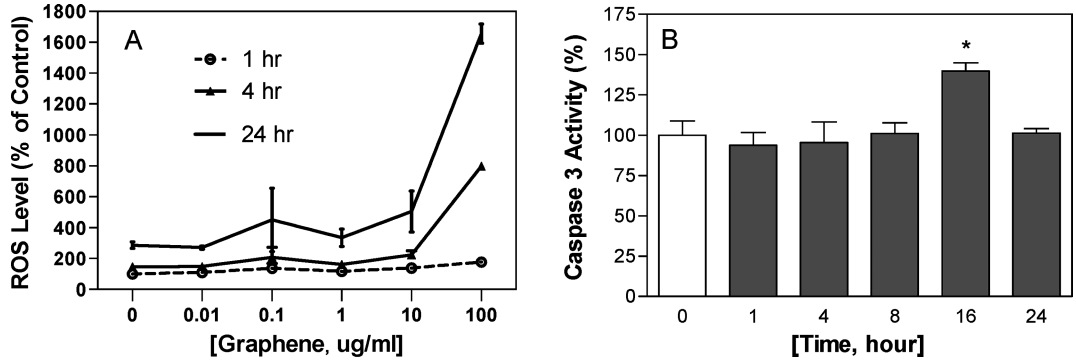

Figure 4. Effect of graphene on (A) ROS generation and (B) caspase 3 activity (apoptosis marker).

of CNT reduced the total DNA content of mixed neuroglial cultures.[28] Other evidence showed that the maximum value of 30 μg/mL of CNT reduced the cell viability and DNA content in human MSTO-211H cells after 3 days of exposure.[29] In our studies, the 100 μg/mL of G increased the LDH release and generation of ROS. However, lower doses of G, such as 0.01 μg/mL, had no effect on metabolic activity, LDH release, and ROS multiple end points. Therefore, lower levels of exposure (<0.01 μg/mL) to G could theoretically be useful in biomedical applications. Future studies will focus on *in vivo* toxicology studies to determine if G could potentially penetrate the blood−brain barrier to affect the central nervous system.

Interestingly, our studies demonstrate that G can elicit concentration-dependent cytotoxicity in PC12 cells and that shape or agglomeration may be important factors to consider. Cytotoxicity involved the oxidative stress mechanism and was also mediated through the apoptosis pathway. Recently, we have shown that nanowired drug delivery enhances the neuroprotective efficacy of compounds, reduces spinal cord edema formation, and improves functional outcome following spinal cord injury in rats.[30]

In conclusion, our studies have clearly demonstrated that the shape of carbonaceous nanomaterials plays an extremely important role in how they interact with cells and potentially other biological systems, such as tissues and organisms. Given their relatively low toxicity compared to that of CNT, we expect that the G nanostructures will be key nanomaterials for treating neurodegenerative diseases by acting as the vehicles of drug and growth factors delivery to neuronal cells. Both G and SWCNT induce cytotoxic effects, and these effects are concentration- and shape-dependent according to our evaluation of various metabolic activities. Lactate dehydrogenase levels were found to be significantly higher for SWCNT as compared to the G samples. Moreover, reactive oxygen species were generated in a concentration- and time-dependent manner after exposure to G, indicating an oxidative stress mechanism. Furthermore, time-dependent caspase 3 (apoptosis marker) activation after exposure to G (10 μg/mL) shows evidence of apoptosis. Together, our data suggest that G, like many other carbon-based nanomaterials such as CNT and fullerene, exhibit oxidative potential in biological systems, with shape playing an important role.

MATERIALS AND METHODS

Graphene Synthesis and Characterization. The Fe−Co/MgO catalyst system with a stoichiometric composition of 2.5:2.5:95 wt % was prepared by the impregnation method as previously shown.[9] Few-layer graphene sheets were grown by radio frequency catalytic chemical vapor deposition (RF-cCVD) on a MgO-supported Fe−Co bimetallic catalyst system utilizing acetylene as a hydrocarbon source. Approximately 100 mg of the catalyst was uniformly spread into a thin layer on a graphite susceptor and placed in the center of a quartz tube with an inner diameter of 1 in. First, the tube was purged with a carrier gas (argon) for 10 min at 150 mL/min. Next, the RF generator (which provides a very fast heating rate of 300−350 °C/min) was turned on to begin heating. When the temperature of the graphite boat reached 1000 °C, acetylene was introduced at 4.5 mL/min for 30 min. At the end of the reaction, the system was cooled under argon for 10 min. The as-produced G sheets were purified in one easy step using diluted hydrochloric acid solution and sonication. Graphene sheets were thoroughly characterized by microscopy, spectroscopy, and X-ray diffraction.

SWNT Synthesis. Carbon nanotubes were synthesized over the Fe−Co/MgO catalyst using the RF-cCVD method and methane as the carbon source.[31] The RF inductive heating was performed using an RF generator operated at 365 kHz. A 200 mg quantity of catalyst was placed in a graphite boat, and the boat was inserted into a quartz reactor. The catalysts were heated in nitrogen (flow rate 600 mL/min) and annealed at 700 °C for 1 h. All of the synthesis reactions were performed at 850 °C with a methane flow rate of 80 mL/min, while keeping the nitrogen flow constant. The temperature of the graphite boat was continuously measured by an optical pyrometer and was found to be very stable during the reaction process. After 30 min of reaction time, the methane was turned off, and the resulting product was allowed to cool in nitrogen flow. The as-produced SWNTs were purified using hydrochloric acid solution. Their diameters were found to range between 0.8 and 1.2 nm, as previously shown.[31]

TEM images were collected on a field emission JEM-2100F transmission electron microscopy (JEOL Inc.) equipped with a CCD camera. The acceleration voltage was 100 kV for the G analysis. The G nanosheets and the nanotube samples were homogeneously dispersed in 2-propanol under ultrasonication for 30 min. Next, a few drops of the suspension were deposited on the TEM grid, dried, and evacuated before analysis.

SEM images were obtained using a JEOL model 7000F high-resolution scanning electron microscope having a resolution of 1.2 nm at an accelerating voltage of 15 kV and a working distance of 10 mm. The final products were mounted on aluminum pins with double-sided carbon tape, and their corresponding SEM images were obtained.

AFM measurements were performed using a Veeco Dimension 3100 atomic force microscope having a scan range of 90 μm for the *x*/*y* direction and 6 μm for the *z* direction. After the G sheets were individually dispersed into 2-propanol solution, a few drops of the final solution were pipetted on Si substrates. Next, the substrates were air-dried and placed directly under the AFM tip for morphology analysis.

Cell Culture. A PC12 cell line was obtained from the American Type Culture Collection (ATCC, Manassas, VA). PC12 cells were maintained at 37 °C (5% CO_2, 95% air) in RPMI-1640 medium (Sigma 8758) supplemented with 5% fetal bovine serum (Atlanta Biologicals), 10% horse serum (ATCC), and 1% penicillin/streptomycin (Sigma). The fresh medium was replaced every other day. Confluent cells were harvested with 0.25% trypsin−EDTA solution (Invitrogen). Before treatment with G nanomaterials, PC12 cells were allowed to attach on 96-well plates for 48 h. The PC12 cells were then exposed to G (0−100 μg/mL) for 24 h. Graphene dilutions were in serum-free, phenol red-free RPMI-1640 medium.

MTT Assay. The colorimetric 3-(4,5-dimethylthiazol-2-yl)-2,5-diphenyltetrazolium bromide (MTT, Sigma) test assesses cell metabolic activity on the basis of the ability of the mitochondrial succinate−tetrazolium reductase system to convert the yellow dye (MTT) to a purple-colored formazan in living cells. The metabolic activity of the cell is proportional to the color density formed. Briefly, following PC12 cell incubation with G or SWCNT for 24 h, the media were aspirated and replaced with 90 μL of serum-free media. To each well was added 10 μL of an MTT stock solution (5 mg/mL), followed by incubation for 4 h at 37 °C. The supernatant was then removed, and cells were lysed with 100 μL of dimethylsulfoxide. Absorbance was recorded at 550 nm using a Synergy 2 microplate reader (Biotek, USA).

Lactase Dehydrogenase Release. Cell membrane integrity can be measured by LDH assay, as the cell was targeted by various agents. LDH activity was measured using a cytotoxicity detection kit from Roche Applied Science. Released LDH in culture supernatants was measured with a coupled enzymatic assay that results in the conversion of a tetrazolium salt (INT) into a red formazan product. PC12 cells (1×10^5 cells/mL) were treated at different concentrations of G or SWCNT nanomaterials for 24 h, then 50 μL of supernatant was removed to another plate, followed by the addition of 50 μL of substrate mix. The plate was covered with foil to protect it from light and incubated for 30 min at room temperature, followed by the addition of 50 μL of stop solution to each well. Absorbance was recorded at 490 nm using a microplate reader (Biotek, USA).

Reactive Oxygen Species Measurement. The ROS level was monitored using DCFH-DA (Molecule Probes Inc., Eugene, OR). The cells were incubated with DCFH-DA (100 μM) in medium for 30 min. PC12 cells (1×10^5 cells/mL) were washed three times with phosphate, buffered in saline solution twice, and then cultured with different concentrations of G. The fluorescence intensity (indicating ROS level) of the cells was determined at 1, 4, or 24 h after the treatment using a microplate reader (Biotek, USA) with excitation/emission at 485/530 nm. The values were expressed as percent of fluorescence intensity relative to control wells. All the procedures were performed without exposure to light.

Caspase 3/7 Assay. Caspase 3/7 is activated in apoptosis. Cells were seeded into 96-well plates (1×10^5 cells/mL) and allowed to attach for 48 h. The cells were exposed to G (10 μg/mL) at different times as indicated. Caspase 3/7 activity was measured 0, 1, 4, 8, 16, and 24 h later. The luminogenic caspase 3/7 substrate containing tetrapeptide sequence DEVD was used for caspase 3/7 cleavage and generation of the luminescent signal based on the standard protocol (Promega, Madison, WI). Briefly, 100 μL of Caspase-Glo3/7 reagent was added to each well, followed by incubation at room temperature for 1 h. The luminescence of each sample was measured using a microplate reader (Biotek, USA).

Evaluation of Morphology Alteration. To evaluate possible changes in cell morphology induced by G or SWCNT in the cell culture, G or SWCNT (10 μM) was incubated with PC12 cells for up to 24 h. Images were captured using a light microscope with a camera at 2, 16, and 24 h.

Statistical Analyses. For continuous responses, data were expressed as mean ± standard error (SE) based on at least triplicate observations from three independent experiments. Statistical significance was determined by one-way analysis of variance (ANOVA) followed by Dunnett's multiple comparison test. A value of $p < 0.05$ was considered statistically significant. All analyses were conducted using the Prism software package (GraphPad Software).

Acknowledgment. This research was supported in part by an appointment (Y.Z.) to the Research Participation Program at the National Center for Toxicological Research, administrated by the Oak Ridge Institute of Science and Education through an interagency agreement between the U.S. Department of Energy and the U.S. Food and Drug Administration. The views presented in this article do not necessarily reflect those of the U.S. Food and Drug Administration. Financial assistance from the Arkansas Science and Technology Authority Grant No. 08-CAT-03 is highly appreciated.

REFERENCES AND NOTES

1. Kim, K. S.; Zhao, Y.; Jang, H.; Lee, S. Y.; Kim, J. M.; Ahn, J. H.; Kim, P.; Choi, J. Y.; Hong, B. H. Large-scale Pattern Growth of Graphene Films for Stretchable Transparent Electrodes. *Nature* **2009**, *457*, 706–710.
2. Han, M. Y.; Oezyilmaz, B.; Zhang, Y.; Kim, P. Energy Band Gap Engineering of Graphene Nanoribbons. *Phys. Rev. Lett.* **2007**, *98*, 206805.
3. Stankovich, S.; Dikin, D. A.; Dommett, G. H. B.; Kohlhaas, K. M.; J., Z. E.; Stach, E. A.; Piner, R.; Nguyen, S. T.; Ruoff, R. S. Graphene-based Composite Materials. *Nature* **2006**, *442*, 282–286.
4. Watcharotone, S.; Dikin, D. A.; Stankovich, S.; Piner, R.; Jung, I.; Dommett, G. H.; Evmenenko, G.; Wu, S. E.; Chen, S. F.; Liu, C. P.; et al. Graphene-silica Composite Thin Films as Transparent Conductors. *Nano Lett.* **2007**, *7*, 1888–1892.
5. Mohanty, N.; Berry, V. Graphene-based Single-bacterium Resolution Biodevice and DNA Transistor: Interfacing Graphene Derivatives with Nanoscale and Microscale Biocomponents. *Nano Lett.* **2008**, *8*, 4469–4476.
6. Sun, X.; Liu, Z.; Welsher, K.; Robinson, J. T.; Goodwin, A.; Zaric, S.; Dai, H. Nano-Graphene Oxide for Cellular Imaging and Drug Delivery. *Nano Res.* **2008**, *1*, 203–212.
7. Colvin, V. L. The Potential Environmental Impact of Engineered Nanomaterials. *Nat. Biotechnol.* **2003**, *21*, 1166–1170.
8. Hussain, M. A.; Kabir, M. A; Sood, A. K. On the Cytotoxicity of Carbon Nanotubes. *Curr. Sci.* **2009**, *96*, 664–673.
9. Dervishi, E.; Li, Z.; Watanabe, F.; Biswas, A.; Xu, Y.; Biris, A. R.; Saini, V.; Biris, A. S. Large-scale Graphene Production by RF-cCVD Method. *Chem. Commun.* **2009**, *27*, 4061–4063.
10. Ferrari, A. C.; Meyer, J. C.; Scardaci, V.; Casiraghi, C.; Lazzeri, M.; Mauri, F.; Piscanec, S.; Jiang, D.; Novoselov, K. S.; Roth, S.; et al. Raman Spectrum of Graphene and Graphene Layers. *Phys. Rev. Lett.* **2006**, *97*, 187401.
11. Graf, D.; Molitor, F.; Ensslin, K.; Stampfer, C.; Jungen, A.; Hierold, C.; Wirtz, L. Spatially Resolved Raman Spectroscopy of Single- and Few-layer Graphene. *Nano Lett* **2007**, *7*, 238–242.
12. Graf, D.; Molitor, F.; Ensslin, K.; Stampfer, C.; Jungen, A.; Hierold, C.; Wirtz, L. Raman Imaging of Graphene. *Solid State Commun.* **2007**, *143*, 44–46.
13. Dimovski, S.; Nikitin, A.; Ye, H.; Gogotsi, Y. Synthesis of Graphite by Chlorination of Iron Carbide at Moderate Temperatures. *J. Mat. Chem* **2004**, *14*, 238–243.
14. Biscoe, J.; Warren, B. A X-Ray Study of Carbon Black. *J. Appl. Phys.* **1942**, *13*, 364–372.
15. Poland, C. A.; Duffin, R.; Kinloch, I.; Maynard, A.; Wallace, W. A.; Seaton, A.; Stone, V.; Brown, S.; Macnee, W.;

Donaldson, K. Carbon Nanotubes Introduced into the Abdominal Cavity of Mice Show Asbestos-like Pathogenicity in a Pilot Study. *Nature Nanotechnol.* **2008**, *3*, 423–428.
16. Warheit, D. B.; Laurence, B. R.; Reed, K. L.; Roach, D. H.; Reynolds, G. A.; Webb, T. R. Comparative Pulmonary Toxicity Assessment of Single-wall Carbon Nanotubes in Rats. *Toxicol. Sci.* **2004**, *77*, 117–125.
17. Sayes, C. M.; Gobin, A. M.; Ausman, K. D.; Mendez, J.; West, J. L.; Colvin, V. L. Nano-C60 Cytotoxicity is Due to Lipid Peroxidation. *Biomaterials* **2005**, *26*, 7587–7595.
18. Sayes, C. M.; Marchione, A. A.; Reed, K. L.; Warheit, D. B. Comparative Pulmonary Toxicity Assessments of C60 Water Suspensions in Rats: Few Differences in Fullerene Toxicity *in vivo* in Contrast to *in vitro* Profiles. *Nano Lett.* **2007**, *7*, 2399–2406.
19. Belyanskaya, L.; Weigel, S.; Hirsch, C.; Tobler, U.; Krug, H. F.; Wick, P. Effects of Carbon Nanotubes on Primary Neurons and Glial Cells. *Neurotoxicology* **2009**, *30*, 702–711.
20. Chan, W. H.; Shiao, N. H.; Lu, P. Z. CdSe Quantum Dots Induce Apoptosis in Human Neuroblastoma Cells via Mitochondrial-dependent Pathways and Inhibition of Survival Signals. *Toxicol. Lett.* **2006**, *67*, 191–200.
21. Lovric, J.; Cho, S. J.; Winnik, F. M.; Maysinger, D. Unmodified Cadmium Telluride Quantum Dots Induce Reactive Oxygen Species Formation Leading to Multiple Organelle Damage and Cell Death. *Chem. Biol.* **2005**, *12*, 1227–1234.
22. Welsher, K.; Liu, Z.; Daranciang, D.; Dai, H. Selective Probing and Imaging of Cells with Single Walled Carbon Nanotubes as Near-infrared Fluorescent Molecules. *Nano Lett.* **2008**, *8*, 586–590.
23. Nel, A.; Xia, T.; Madler, L.; Li, N. Toxic Potential of Materials at the Nanolevel. *Science* **2006**, *311*, 622–627.
24. Shi, L.; Hernandez, B.; Selke, M. Singlet Oxygen Generation from Water-soluble Quantum Dot−Organic Dye Nanocomposites. *J. Am. Chem. Soc.* **2006**, *128*, 6278–6279.
25. Wang, J.; Rahman, M. F.; Duhart, H. M.; Newport, G. D.; Patterson, T. A.; Murdock, R. C.; Hussain, S. M.; Schlager, J. J.; Ali, S. F. Expression Changes of Dopaminergic System-related Genes in PC12 Cells Induced by Manganese, Silver, or Copper Nanoparticles. *Neurotoxicology* **2009**, *30*, 926–933.
26. Hussain, S. M.; Javorina, A. K.; Schrand, A. M.; Duhart, H. M.; Ali, S. F.; Schlager, J. J. The Interaction of Manganese Nanoparticles with PC-12 Cells Induces Dopamine Depletion. *Toxicol. Sci.* **2006**, *92*, 456–463.
27. Lam, C. W.; James, J. T.; McCluskey, R.; Hunter, R. L. Pulmonary Toxicity of Single-wall Carbon Nanotubes in Mice 7 and 90 Days after Intratracheal Instillation. *Toxicol. Sci.* **2004**, *77*, 126–134.
28. Belyanskaya, L.; Weigel, S.; Hirsch, C.; Tobler, U.; Krug, H. F.; Wick, P. Effects of Carbon Nanotubes on Primary Neurons and Glial Cells. N. *eurotoxicology* **2009**, *30*, 702–711.
29. Wick, P.; Manser, P.; Limbach, L. K.; Dettlaff-Weglikowska, U.; Krumeich, F.; Roth, S.; Stark, W. J.; Bruinink, A. The Degree and Kind of Agglomeration Affect Carbon Nanotube Cytotoxicity. *Toxicol. Lett.* **2007**, *168*, 121–131.
30. Sharma, H. S.; Ali, S. F.; Ryan, T. Z.; Patnik, R.; Patnik, S.; Sharma, A.; Boman, A.; Per, L.; Seifert, E.; Torbjorn, L. Nanowired-drug Delivery Enhances Neuroprotective Efficacy of Compounds and Reduces Spinal Cord Edema Formation and Improves Functional Outcome Following Spinal Cord Injury in the Rat. *Acta Neurochirurgica* **2010**, *106*, 343–350.
31. Xu, Y.; Li, Z.; Dervishi, E.; Saini, V.; Cui, J.; Biris, A. R.; Lupu, D.; Biris, A. S. Surface Area and Thermal Stability Effect of the MgO Supported Catalysts for the Synthesis of Carbon Nanotubes. *J. Mater. Chem.* **2008**, *18*, 5738–5745.